HATS GC-ECD Analysis of Flask Samples on "Otto"

J. David Nance, April 2015

The HATS group has used a three-channel gas chromatograph with electron capture detectors (GC-ECD) nicknamed "Otto" in the analysis of air samples collected in stainless steel and glass flasks from globally distributed sites since 1995. Analyzed peaks include N_2O, SF_6, CFC-11, CFC-12, CFC-113, CH_3CCl_3 and CCl_4. Otto's sampling protocol involves alternating injections between atmospheric flask samples and calibration gases stored in high-pressure cylinders called "standards". After interpolating standard-gas ("*S*") responses to the injection times for flask-air ("*A*"), a quick estimate of the atmospheric concentration can be obtained from

$$\hat{C}_A = R_A \frac{dC}{dR}, \qquad \frac{dC}{dR} \cong \frac{C_S}{R_S} \tag{1}$$

Here, C and R, respectively, are the concentration of, and GC system response to, the sample sources signified by the subscripts. This simple formula relies on a single standard to estimate the response function of the GC with a line through [C_S, R_S] and [0, 0]. Another way of thinking about (1) is that the atmospheric concentration can be estimated by multiplying the standard-gas concentration by the standard-gas-normalized flask-air response. This simple method can offer good quality C_A estimates when the true response function is a straight line. Otherwise, C_A must be very close to C_S. In practice, GC-ECD response functions often show some evidence of curvature, and the distance between C_A and C_S changes with the flask sampling location and at the rate of the overall atmospheric trend during a standard's duty cycle.

When the response function is not a straight line, a better local estimate of *dC/dR* in the vicinity of C_A can be obtained with the addition of a second standard. In a world of perfect measurements, we would ideally want the concentration of both standards to be as close to C_A as possible in order to create a perfect tangent line to the response curve at C_A. In the world of noisy measurements, this would only create a virtual pivot point about which the local *dC/dR* estimate would fluctuate wildly. So efforts are made to separate the second standard by an optimal distance that nicely balances the competing goals of reducing the noise of the *dC/dR* estimate to acceptable levels while still keeping the standard-gas concentrations close enough to C_A to give an adequately local estimate of *dC/dR*.

All of our tertiary standards are filled with background air at Niwot Ridge, CO, and our approach with all two-standard GC systems, including Otto, is to have one standard ("*S2*") holding background air and the other standard ("*S1*") holding background air diluted with ~10% "zero air" – a typical mixture of N_2, O_2, and Ar scrubbed of other contaminants. Alternating between flask-air and standard-gas injections and further alternating standard-gas injections between *S1* and *S2* now allows a second estimate of C_A using a two-standard formula:

$$\hat{C}_A = C_{S1} + \left(R_A - R_{S1}\right)\frac{dC}{dR}, \qquad \frac{dC}{dR} \cong \frac{C_{S2} - C_{S1}}{R_{S2} - R_{S1}} \tag{2}$$

The second standard also allows an additional estimate of C_A from (1).

With precise measurements, all three estimates would agree when the response function is a straight line. In practice, the three estimates almost never agree, not only because GC-ECD response functions tend to be curved and measurements tend to be noisy, but also because GC responses are influenced by systemic biases that manifest differently from one GC to the next. Moreover, biases often arise from trace contaminants that vary from one standard to the next.

The tertiary standards used by Otto are defined in reference to calibration scales derived from secondary standards analyzed in our Standards Lab on a separate GC-ECD system. (The secondary standards are defined in reference to primary calibration scales derived from valuable gravimetric standards that are used more sparingly.) Unlike Otto, the Standards GC generates a calibration scale by running a polynomial fit through its normalized responses to a broad range of concentrations from secondary standards such that any response biases associated with the individual secondary standards are smoothed over by the fit. In contrast, the finite differencing scheme embedded in (1) and (2) exposes C_A estimates from the two-standard Otto system to the full effects of all systemic response biases and random measurement noise specific to Otto and the tertiary standards it uses. These biases have the potential to significantly distort the *dC/dR* estimates of (1) and the much more local *dC/dR* estimates of (2) even more so.

In an effort to improve this situation, a method was developed for modifying (1) and (2) to incorporate information derived from a systematic review of all standard-gas measurements throughout Otto's history. In effect, this method extends Otto's calibration scales beyond the two standards being run at any given time by using the measurements from all standards to estimate and account for a) the curvatures of Otto's various peak response functions, and b) any response biases that may be associated with the individual standards. We began reporting flask GC-ECD measurements from Otto using this reduction method in 2009.

Before any standards-specific bias adjustments can be derived, a quantitative assessment of the curvatures of Otto's response functions is required. Since response tends to float around over time even for well-controlled GCs, we will use Otto's standard-gas responses to normalize each other and compare how the normalized response – i.e. the response ratio – varies in accordance with the ratio of concentration values determined using the Standards GC. Figure 1 (figures are at the back end of this document) shows an historical time series of *S1*/*S2* response ratios for CFC-113 from standards injections on Otto. Over much of this series, the concentration ratio lines are separated from the median response ratio lines in rough proportion to their distance from unity, a clear sign of response function curvature.

Looking ahead, it will be desirable to extend this initial set of ratios while maximizing the linkages between them. When standards are cycled on and off one at a time, each standard is partnered with at least two others to produce an interconnected system of directly measured response ratios. With some awareness of the overall trend across an atmospheric time series, flask-air samples from individual stations may be used as common – though admittedly non-constant/trending – normalizing parameters to indirectly derive mean response ratios between sequentially adjacent standards. This process involves finding a S_i/S_j response ratio that will bring adjacent A/S_i and A/S_j response ratio series into appropriate alignment consistent with the

overall atmospheric trend (here, the *i* and *j* subscripts designate arbitrary standards, as signified, for example, by the identifier codes shown in figure 1). Such estimates are vulnerable to the introduction of subjective bias. However, the availability of flask-air samples from multiple stations helps to mitigate this concern by making the process less selective and more statistical. The end effect is to extend the interconnections across the entire set of standards by bridging across transitions where both standards were cycled simultaneously. Finally, response ratios between standards far removed in time can also then be indirectly estimated by methodically multiplying through chains of more directly measured ratios so that all but two standards at the endpoints cancel out. The final result will be a single interconnected system of tertiary standards, where each standard is involved in a ratio expression with every other standard. In the case of CFC-113, these response and concentration ratios are plotted along with their inverses in figure 2a after logarithmic transformation to balance the opposing lobes.

Because of the symmetry between the lower left and upper right quadrants of figure 2a, a linear fit through the data will always pass directly through the origin and take the form of a simple slope with zero intercept. The curvature of the CFC-113 response curve is gauged by the deviation of this slope from 1. Since we are interested in estimating concentration as a function of GC response, the response ratio was placed on the x-axis and the concentration ratio on the y-axis. Within this orientation, a slope > 1 is indicative of a flattening response function for a sub-sensitive GC becoming less responsive as concentration increases. Conversely, a slope < 1 would be indicative of a steepening response function for a super-sensitive GC becoming more responsive as concentration increases. A slope ≈ 1, meanwhile, would signify an essentially linear response function for an optimally sensitive GC.

The spread of the data about the fitted line is assumed to correlate primarily with the presence of systemic biases in Otto's response to the individual standards, although it may also to some extent reflect errors in the concentration values determined for the standards using the Standards GC. Such errors would presumably result from small biases in the Standards GC's response to the same tertiary standards. These biases may result from random noise in the measurements, or they may originate from transient, systemic errors that migrate through the GC over time. It has, for example, been observed that small but significant differences between concentration estimates for the same tertiary standard may appear when new samples are injected on the Standards GC after an interval of several days. Finally, the Standards GC, like Otto, is an autonomous system. It columns, detectors, and other components, and its program for controlling the flow of samples through the system are unique to itself, and the chromatograms it produces have their own unique features that are distinct from those of Otto. We should therefore not expect Otto's measured responses to these standards to be precisely consistent with the concentrations determined using the Standards GC.

To compensate for standards-specific response biases, two approaches are available: 1) derive a set of standards-specific proportionality constants (i.e. multiplication factors) that adjust Otto's drifting response to the standards to be more consistent with the concentrations defined by the Standards GC; or 2) derive a set of constant offsets that adjust the standards concentrations to be more consistent with the response values from Otto. For reasons that will not be detailed here, the second approach is less complicated to execute. Be cautioned, however, that while adjusting the standards concentrations might seem to imply that the Standards GC is the primary source of

bias – just as adjusting Otto's responses to its standards might likewise seem to imply that Otto is the primary source of bias – in truth both sources are inextricably combined and compensated for by either approach. So, while we will be deriving adjustments for the standards concentrations, the results will certainly not be exclusively reflective of the quality of the tertiary standards concentrations defined by the Standards GC. They may, in fact, be significantly more reflective of Otto's unique response characteristics, but in any case, this technique will not distinguish between the two influences. We have chosen to adjust the standards concentrations simply as a matter of convenience.

The following is an equation describing any single data point shown in figure 2a in terms of the fitted line:

$$\log_e\left(C_i/C_j\right) = m \times \log_e\left(\overline{R_i/R_j}\right) + \hat{\varepsilon}_{ij} \tag{3}$$

where m is the slope of the fit and $\hat{\varepsilon}_{ij}$ is the residual of the concentration ratio for standards i and j. We want to find a pair of standard-gas concentration offsets, δ_i and δ_j, that will make the residual go away:

$$\log_e\left(\frac{C_i + \delta_i}{C_j + \delta_j}\right) = m \times \log_e\left(\overline{R_i/R_j}\right) \tag{4}$$

Exponentiating (4) and rearranging terms gives an expression of the following linear form:

$$a_i\delta_i + a_j\delta_j = b\ , \tag{5}$$

where

$$a_i = 1\ , \qquad a_j = -\left(\overline{R_i/R_j}\right)^m\ , \qquad b = C_j\left(\overline{R_i/R_j}\right)^m - C_i \tag{5a, b, c}$$

Since each standard is involved in a ratio expression with every other standard, the concentration offset determined for any single standard is required to satisfy multiple expressions of (5) simultaneously. The resulting linear system has *nstd* unknown δ values, and $neqn = \sum_{n=1}^{nstd-1} n$ ratio expressions:

$$\mathbf{A} \cdot \mathbf{x} = \mathbf{b}\ , \tag{6}$$

$$\mathbf{A} = \begin{bmatrix} a_{1,1} & a_{1,2} & \cdots & a_{1,nstd} \\ a_{2,1} & a_{2,2} & \cdots & a_{2,nstd} \\ \vdots & \vdots & \ddots & \vdots \\ a_{neqn,1} & a_{neqn,2} & \cdots & a_{neqn,nstd} \end{bmatrix}, \qquad \mathbf{b} = \begin{bmatrix} b_1 \\ b_2 \\ \vdots \\ b_{neqn} \end{bmatrix}, \qquad \mathbf{x} = \begin{bmatrix} \delta_1 \\ \delta_2 \\ \vdots \\ \delta_{nstd} \end{bmatrix} \tag{6a, b, c}$$

Note that **A** is a sparse matrix with only two nonzero coefficients, a_i and a_j, on each row.

Least squares solutions to overdetermined linear systems of this sort are attainable via the singular value decomposition of **A** (see, for example, Press et. al., section 2.6) to produce a trio of component matrices:

$$\mathbf{A} = \mathbf{U} \cdot \mathbf{W} \cdot \mathbf{V}^T \tag{7}$$

Here, **U** is column orthogonal and dimensioned identically to **A** (*neqn* x *nstd*), **V** is also orthogonal but square (*nstd* x *nstd*), and **W** is the *nstd* x *nstd* diagonal matrix of singular values (the columns of **U** and **V** are said to hold the left-hand and right-hand singular vectors of **A)**. All three are easily inverted – by taking the transpose of the orthogonal matrices **U** and **V**, and by simply inverting the diagonal values of **W**. A solution that minimizes the size of the residual vector, $\|\mathbf{A} \cdot \mathbf{x} - \mathbf{b}\|$, and the size of the solution vector itself, $\|\mathbf{x}\|$, is computed from

$$\mathbf{x} = \mathbf{V} \cdot \mathbf{W}^{-1} \cdot \left(\mathbf{U}^T \cdot \mathbf{b}\right) \tag{8}$$

An examination of (5) will reveal that $\|\mathbf{A} \cdot \mathbf{x} - \mathbf{b}\|$ can be minimized all the way to zero when $\delta = -C$ so that $C + \delta = 0$. A consequence of this is that there will always be a solitary singular value on the diagonal of **W** that is several orders of magnitude below the rest. This isolated singular value dwarfs the others when **W** is inverted, and it must be zeroed out prior to the computation of **x** by (8) to block a linear combination that ignores the ratio data and pushes the result toward this exact, but trivial, solution (refer again to Press et. al. section 2.6). The alternative result will ideally be a set of much smaller δ values that are more or less evenly distributed about zero (figure 2b).

Ideal outcomes are commonly precluded when one or more δ values stands out in terms of its magnitude. The balancing mechanism implied by the minimization of $\|\mathbf{x}\|$ then pushes the other δ values toward the opposite side of zero. To prevent these discordant standards from biasing the δ values derived for their more congruent counterparts in this fashion, it will be necessary to remove them from the linear system and solve again. Care must also be taken at the outset to identify and remove from the system standards that show signs of such significant instability during their duty cycles that they would ultimately be ignored in the final analysis. In figure 2, the two *S2* standards at the endpoints have been removed from the linear system, along with the first two *S1* standards and *S1* standard 52750a, and all ratio data and estimated offsets associated with these standards have been marked with gray circles.

With the subset of high-quality standards that remains, the initial set of δ values can be used to derive "precisions" to weight the C_i/C_j ratios in figure 2 and refit with a new line. The new fit will produce a different set of residuals to be compensated for with a new set of δ values. This process can be iterated until the fit converges on a slope that is weighted toward ratios of the highest-quality standards with the smallest δ values. (Note: be careful to set a floor precision on the concentration ratios – the median value, for example – to prevent the fit from quickly homing in on a single concentration ratio relating the two standards whose δ values are closest to zero at the initial iterative step.) When the slope of the fit is finalized, δ values for those isolated standards with large or unstable response biases can be estimated directly from (5) using ratio expressions in which they participate with high-quality standards that already have δ values.

These finalized parameters can be used to amend (1) and (2) for the recomputation of atmospheric concentrations from the Otto measurements. After appropriately transforming (4), the new single-standard estimating function becomes

$$\hat{C}_A = \left(C_S + \delta_S\right)\left(R_A / R_S\right)^m \tag{9}$$

Here, m adjusts the standard-gas-normalized flask-air response to compensate for the curvature of the response function, and δ_S adjusts C_S to a value that better conforms with R_S in consideration of Otto's aggregate response to all of its standards. The new two-standard function comes simply from adding δ_{S1} and δ_{S2} to the *S1* and *S2* concentration values:

$$\hat{C}_A \cong \left(C_{S1} + \delta_{S1}\right)\left(R_A - R_{S1}\right)\frac{dC}{dR}\,, \qquad \frac{dC}{dR} \cong \frac{\left(C_{S2} + \delta_{S2}\right) - \left(C_{S1} + \delta_{S1}\right)}{R_{S2} - R_{S1}} \tag{10}$$

When δ_{S1} and δ_{S2} are of significant proportion relative to $C_{S2} - C_{S1}$ and of opposite sign, they can have a sizable impact on the localized dC/dR estimate from (10).

Accordingly, m and the δ values derived from the entire set (or high-quality subset) of Otto standards carry information from that larger set to every measurement on what is otherwise a two-standard system. As long as the δ values for the high-quality set of standards are fairly evenly distributed about zero, then the overall time series of atmospheric measurements from Otto will remain consistent with the calibration scale for tertiary standards set by the Standards Lab. CFC-113 concentrations of flask-air samples from Mauna Loa analyzed on Otto and estimated using equations (1), (2), (9) and (10) are shown in figure 3 to demonstrate the level of convergence achieved between estimates based on the amended versions of the single-standard (with *S1* and *S2* used independently) and two-standard functions.

To facilitate a brief discussion of figure 3, single-standard flask-air estimates from equation (1) that are referenced to the *S1* standards will be referred to as the *S1-cal* calibration, single-standard estimates from equation (1) that are referenced to the *S2* standards will be referred to as the *S2-cal*, and two-standard equation (2) estimates will be referred to as the *S1-S2-cal*. Estimates from equations (9) and (10) will be referred to in likewise fashion as the *S1-cal+*, the *S2-cal+*, and the *S1-S2-cal+* calibrations.

In figure 3, the pale-green *S1-S2-cal* dots are sized small to enhance the visibility of the larger pale-blue *S2-cal* dots that are largely hidden beneath them. The overlap is a manifestation of the atmospheric concentrations being much closer to the background *S2* concentrations than to the diluted-background *S1* concentrations. This mitigates the effect of response function curvature on the *S2-cal* and places heavier emphasis on the *S2* reference point in the *S1-S2-cal*. In contrast, the greater relative distance between the atmospheric and *S1* concentrations amplifies the *S1-cal* error that is due to response function curvature and promotes the tendency for the *S1-cal* (pale-red dots) to underestimate the *S2-cal* and *S1-S2-cal*. Also, even with the close proximity between flask-air and *S2* concentrations, we still see significant shifts in the *S2-cal* and *S1-S2-cal* estimates at *S2* transitions. These shifts are predominantly related to varying biases in Otto's response to these standards.

All of these distortive effects are nicely compensated for by the addition of *m* and the δ values to the estimating functions. From 1999 onward, most of the difference between the *S1-cal* and the *S1-cal+* is accounted for by *m*, with only relatively small δ_{S1} having been derived for these standards (unstable *S1* standard 52750a excepted). In contrast, the impact of *m* on the *S2-cal+* is minimized by the similarity between the atmospheric and *S2* concentrations, while the relatively large δ_{S2} account for most of the difference between the *S2-cal* and *S2-cal+*. The δ_{S2} also account for most of the difference between the *S1-S2-cal* and the *S1-S2-cal+* due to the heavier emphasis placed on the *S2* reference point. Any remaining disagreements are directly tied to the instability of Otto's responses to its standards, which is generally very mild with notable exceptions. The level of agreement achieved between the amended estimates allows these exceptions – *S1* standard 52750a and *S2* standard 73157 – to be more easily excluded from the final analysis in favor of their more competent, opposite partners.

References

Press, W. H., S. A. Teukolsky, W. T. Vetterling, B. P., Flannery (2002), *Numerical Recipes in C++*, Cambridge University Press, New York, NY

Figures

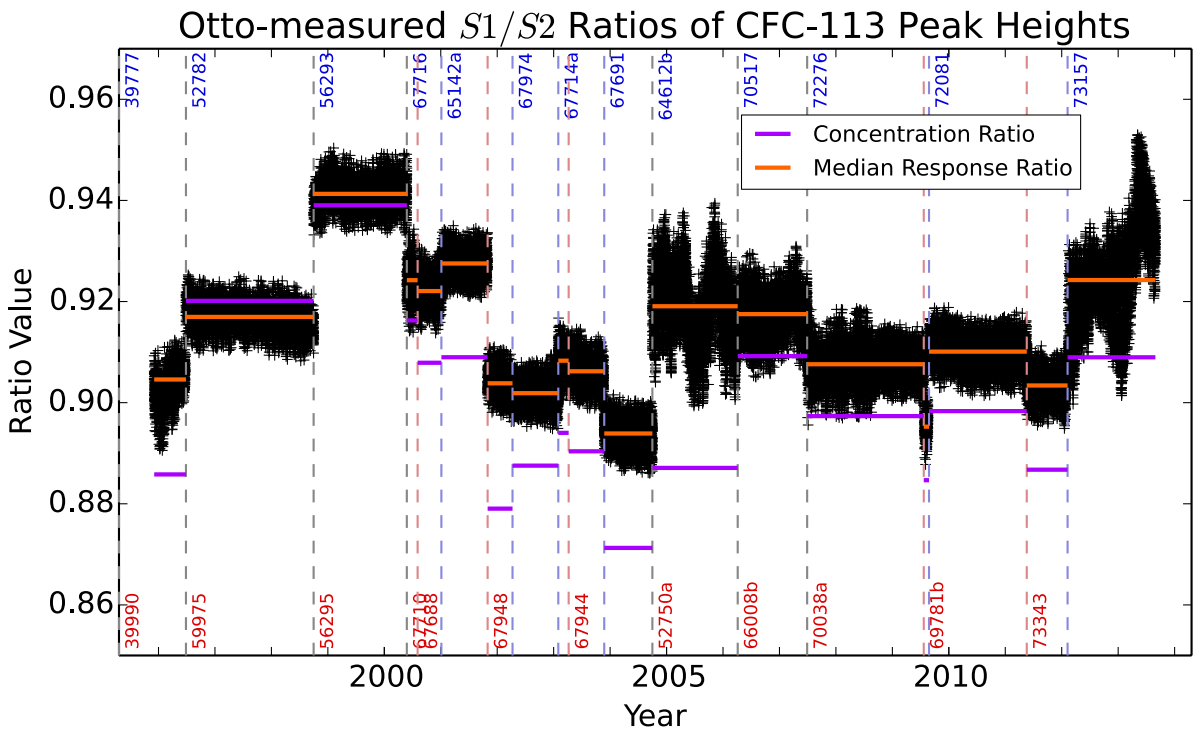

Figure 1. *S1/S2 ratios of CFC-113 responses from standards injections on Otto (black pluses). Individual values are obtained by interpolating responses from alternating injections. For illustrative clarity, these data have been filtered to remove the noisiest values. Dashed, blue vertical lines mark transitions between background S2 standards with blue ID #s listed across the top; dashed, red vertical lines mark transitions between diluted-background S1 standards with red ID #s listed across the bottom; dashed, gray vertical lines indicate where both standards were cycled simultaneously. Horizontal orange lines show the median S1/S2 response ratios for concurrently-running standard pairs, while horizontal purple lines show the associated S1/S2 ratios of concentrations determined by the Standards Lab. Meandering response ratios spanning the year 2005 and since very early in the year 2012 are respectively related to significant instabilities in Otto's response to S1 standard 52750a and S2 standard 73157.*

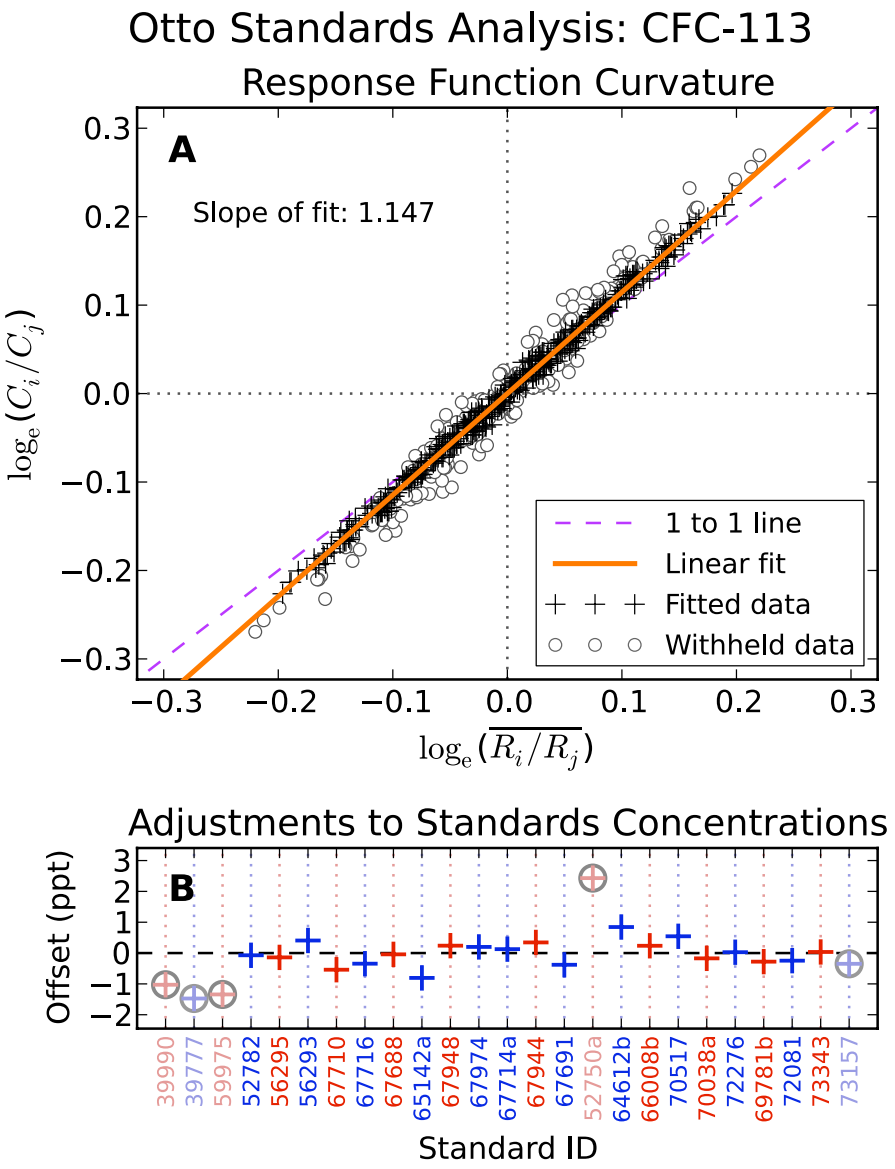

Figure 2. *CFC-113 concentration ratios versus median response ratios from Otto standards after logarithmic transformation (**A**). All possible standard pairs are represented twice in inverted forms. The solid orange line represents a weighted linear fit to the data depicted as black plus marks, with the dashed, purple 1 to 1 line provided for reference. The deviation of the slope from 1 quantifies the magnitude of the curvature in Otto's response function. A set of standards-specific bias adjustments in the form of constant offsets to the standards concentrations is derived in an iterative fashion (refer to text) via equation (6) to compensate for the residuals of the fit (**B**). The gray circles in both panels mark data points associated with standards that were withheld from equation (6). 52750a and 73157 were withheld because of their instability, while 39990, 39777, and 59975 were withheld due to the relative magnitude and general discontinuity of their offsets in comparison with those of the remaining standards. Offsets for these withheld standards were determined using equation (5) after the fit was finalized.*

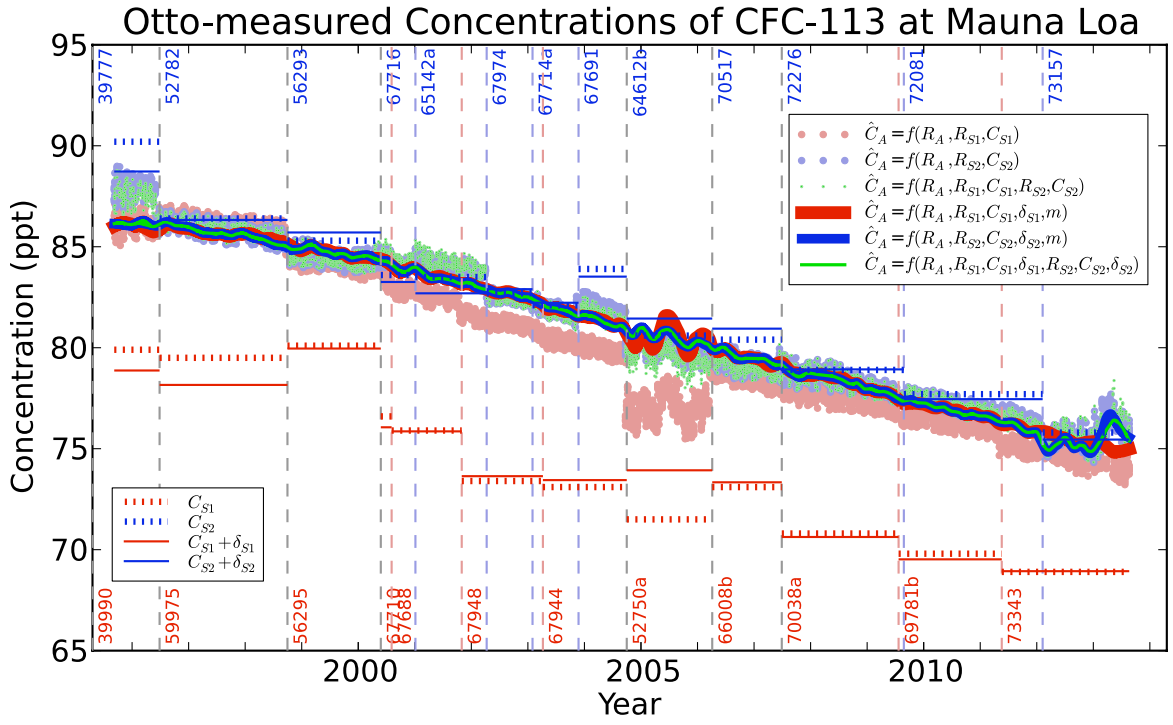

Figure 3. *CFC-113 concentrations at Mauna Loa computed six different ways. Transitions between standards are depicted as in figure 1. Standards concentrations of CFC-113 as determined by the Standards Lab with and without the bias adjustments of figure 2 added are respectively depicted by the horizontal solid and dotted lines spanning the standards' duty cycles. Pale-red dots show C_A estimates computed via equation (1) with respect to the diluted-background S1 standards. Pale-blue dots show those computed via equation (1) with respect to the background S2 standards. Small, pale-green dots were computed via equation (2) with respect to both standards. These data have been filtered of noisy values to facilitate comparison. The slope and offsets derived in figure (2) were used to recompute flask-air concentrations using the amended estimating functions of equations (9) and (10). Soft loess curves were fit through the new estimates and are represented by analogously colored lines of varying thickness to enhance their visibility and comparison with each other and with the original estimates of equations (1) and (2). With exceptions made for estimates based on unstable standards 52750a (S1) and 73157 (S2), the controversies have essentially been eliminated.*